Electronic Supplementary Information for

Layered double hydroxide assembled on g-C_3N_4 modified hollow carbon sphere as adsorbent for removing uranium (VI)†

Xiaoyu Yuan,[a,b,c] Xiaoyan Jing,[a] Jing Yu,[a,c]* Hongsen Zhang,[a,c] Rongrong Chen,[a,c,d] Shouzheng Su,[c,e] Qi Liu,[a,c,g] Milin Zhang[a,f] and Jun Wang[a,c,d,g]*

a. Key Laboratory of Superlight Materials and Surface Technology, Ministry of Education, Harbin Engineering University, Harbin 150001, China

b. College of Materials and Chemical Engineering, Heilongjiang Institute of Technology, Harbin 150050, China

c. College of Materials Science and Chemical Engineering, Harbin Engineering University, Harbin 150001, China

d. Institute of Advanced Marine Materials, Harbin Engineering University, 150001, China.

e. College of Nuclear Science and Technology, Harbin Engineering University, 150001, P. R. China.

f. College of Science, Heihe University, Heihe 164300, China

g. Harbin Engineering University Capital Management Co. Ltd, Harbin 150001, China.

ESI.1 Preparation of SiO_2@RFP

Typically, 0.6 g as-prepared SiO_2 spheres was homogeneously dispersed in 53 mL ultrapure water and 21 mL ethanol by ultrasonication. 0.27 g resorcinol, 1.7 g cetyltrimethyl ammonium bromide and 0.1 mL of ammonia (25%-28%) were added to the SiO_2 suspension in sequence and stirred for 30 min at 35 ^oC. Subsequently, 0.4 mL formaldehyde was added into the mixture, stirring was continued for 6 h, and aged for 12h at room temperature. The resulting SiO_2@RFP microspheres were obtained by centrifugation, washing and drying at 60 ^oC.

ESI.2 Chemicals

Tetraethoxysilane (TEOS) was obtained from the Aladdin. Methanol, ethanol, formaldehyde, ammonia (25%-28%) and urea were purchased from Fuyu Fine Chemical Co. Ltd. Melamine (MA), aluminum isopropoxide ($Al(OPr)_3$), cetyltrimethyl ammonium bromide (CTMAB) and $Ni(NO_3)_2{\cdot}6H_2O$ were obtained from Sinopharm Chemical Reagent Co. Ltd. $UO_2(NO_3)_2{\cdot}6H_2O$ (99.99%) was purchased from Sigma-Aldrich. All of the chemical agents were used without any further purification.

ESI.3 Characterization

Nitrogen adsorption-desorption was evaluated at 77 K using an autoadsorption system (Micromeritics ASAP 2010, America). Degassing of the sample was performed at 393K for 4 h before adsorption measurements. The pore size distributions and Brunauer-Emmet-Teller specific surface area (S_{BET}) were calculated by using the Barrett-Joyner-Halenda (BJH) and Brunauer-Emmet-Teller (BET) methods, respectively. U(VI) concentration at mg L^{-1} or μg L^{-1} level was tested by Inductively Coupled Plasma-Atomic Emission Spectroscopy (ICP-AES, iCAP 7000, America Thermo Scientific) or Inductive Coupled Plasma-Mass Spectrometry (ICP-MS, iCAP RQ, America Thermo

Scientific). The XRD patterns, which recorded on a Rigaku TTR-III diffractometer (Japan) with Cu Kα irradiation (λ = 0.15406 nm), were characterized crystal structures of the target. The microstructures of LDH FHS, C_3N_4-HCS and C_3N_4-HCS@LDH were depicted using a transmission electron microscope (TEM, JEOL 2010, 200 kV, Japan). The measurements of Fourier transform infrared (FT-IR) spectra were conducted on an AVATAR 360 FT-IR spectrophotometer (America) in the 400-4000 cm^{-1} region by the KBr-disk method. X-ray photoelectron spectroscopy (XPS) measurements were performed using a PHI 5700 ESCA spectrometer with Al Kα radiation (America, hν= 1486.6 eV).

ESI.4 Adsorption experiments

The adsorption capacity Q_e ($mg \cdot g^{-1}$) and the removal rate (R) of U(VI) were calculated using **Eqs. (1)** and **(2)**:

$$Q_e = \frac{(C_0 - C_e)}{m} \times V \quad (1)$$

$$R = \frac{(C_0 - C_e)}{C_0} \times 100\% \quad (2)$$

Where V and m are the volume of the solution (L) and the weight of adsorbent (g), respectively. C_0 is the initial U(VI) concentration ($mg\ L^{-1}$), and C_e is the equilibrium U(VI) concentration ($mg\ L^{-1}$).

ESI.5 Characterization of adsorbent

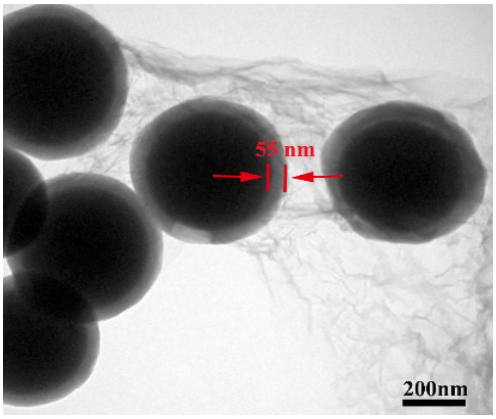

Fig. S1 TEM image of SiO_2@C_3N_4-C.

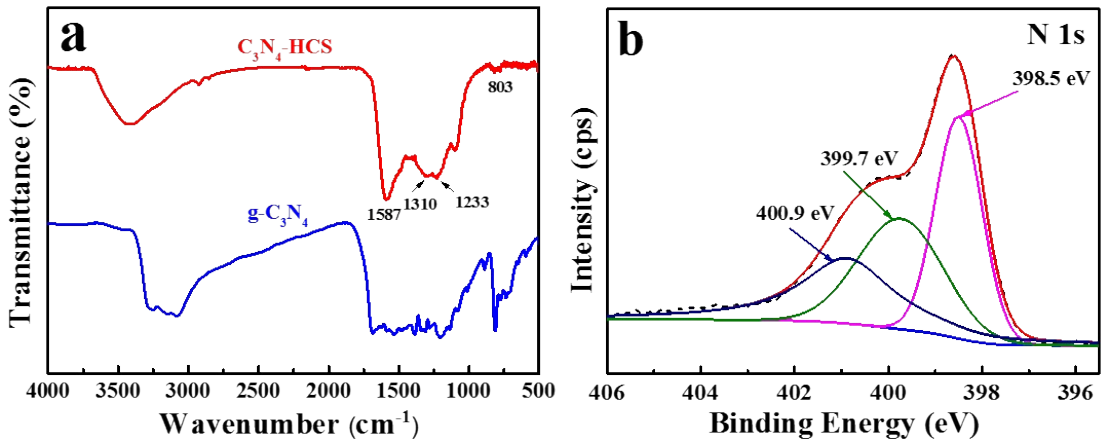

Fig. S2 FT-IR spectra of the C_3N_4-HCS and g-C_3N_4 (a), and XPS of the N 1s high-resolution spectra of the C_3N_4-HCS (b).

ESI.6 Zeta potentials

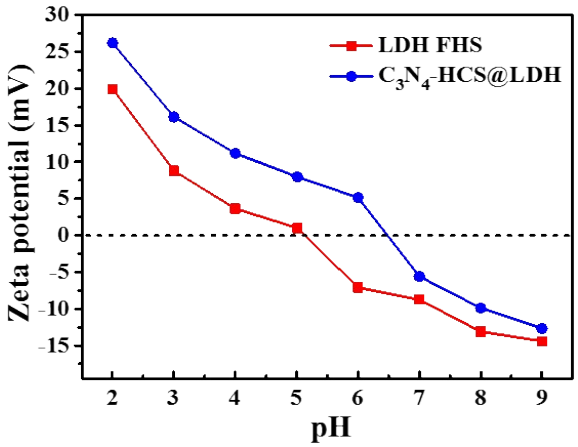

Fig. S3 Zeta potentials of C_3N_4-HCS@LDH and LDH FHS.

ESI.7 Adsorption kinetics

Suggesting that the adsorption was controlled by the diffusion step, the pseudo-first-order model kinetic equation expressed as:

$$\ln\left(Q_e - Q_t\right) = \ln Q_e - k_1 t \quad (3)$$

Assumption that the adsorption process was based on the chemical adsorption mechanism and the pseudo-second-order model equation was written as:

$$\frac{t}{Q_t} = \frac{1}{k_2 Q_e^2} + \frac{t}{Q_e} \quad (4)$$

Where k_1 (min^{-1}) and k_2 (mg g^{-1} min^{-1}) were the adsorption rate constants of the pseudo-first-order and pseudo-second-order models, respectively. Q_t (mg g^{-1}) and Q_e

(mg g^{-1}) are the amounts of adsorbed U(VI) at time t (min) and at the sorption equilibrium, respectively.

On the premise of neglecting the liquid film diffusion resistance, the equation based on the Weber-Morris kinetics model was described as follows:

$$Q_e = k_p\sqrt{t} + C \quad (5)$$

Where k_p (mg g^{-1} $min^{-1/2}$) was the intra-particle diffusion rate constant. C (mg g^{-1}) was a constant describing of the boundary-layer effects.

Table S1 Parameters of intra-particle diffusion kinetics model (T = 298 K).

Materials	first stage		second stage		third stage	
	kp_1	R^2	kp_2	R^2	kp_3	R^2
LDH FHS	11.095	0.991	6.065	0.985	-0.072	0.981
C_3N_4-HCS@LDH	17.732	0.995	7.187	0.947	-0.315	0.909

ESI.8 Adsorption isotherms and thermodynamics

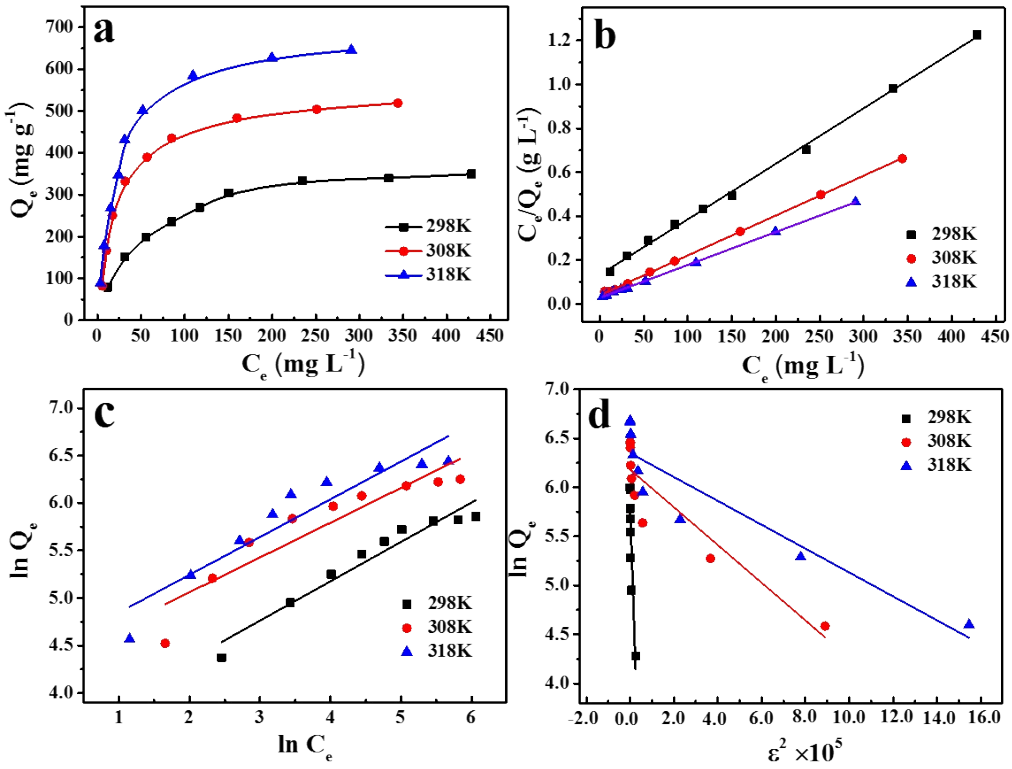

Fig. S4 The adsorption isotherms (a), Langmuir (b), Freundlich (c) and Dubinin-Radushkevich models (d) of LDH FHS (pH = 7.0, V = 20 mL, m = 0.01 g, C_0 = 50-600 mg L^{-1}).

Table S2 Comparison of the U(VI) extraction capacity of C_3N_4-HCS@LDH composite other related materials.

Sorbents	Q_{max} (mg g^{-1})	t (h)	pH	m/V (g L^{-1})	C_0 (mg L^{-1})	Refs.
magnetic Mg-Al LDH	180.0	4.0	6.0	1.0	200	[1]
Fe_3O_4@C@Ni-Al LDH	174.1	3.0	6.0	1.0	200	[2]
PAN-PEI/LDH	554.0	1.5	7.0	0.4	220	[3]
nZVI/C	186.9	10.0	4.0	0.2	10	[4]
CS	79.5	6.0	5.0	0.22	41	[5]
LDH	112.3	8.0	5.0	0.22	41	
porous g-C_3N_4	149.7	2.0	5.0	0.2	60	[6]
Fe_3O_4@g-C_3N_4	352.1	2.5	10.0	1.3	140	[7]
C_3N_4-HCS@LDH	609.7	4.0	7.0	0.5	400	This study

The Langmuir, Freundlich and D-R models are described as:

$$\frac{C_e}{Q_e} = \frac{1}{bQm} + \frac{C_e}{Q_m} \quad (6)$$

$$\ln Q_e = \ln k + \frac{1}{n}\ln C_e \quad (7)$$

$$\ln Q_e = \ln Q_{DR} - \beta\varepsilon^2 \quad (8)$$

$$\varepsilon = RT\ln(1 + 1/C_e) \quad (9)$$

Where Q_m (mg g^{-1}) is the maximum adsorption amount at complete monolayer coverage, C_e (mg L^{-1}) and Q_e (mg g^{-1}) are the U(VI) concentration and experimental adsorption capacity at equilibrium, respectively. b is a constant related to the affinity and energy of adsorbents, k is a Freundlich constant and $1/n$ is associated with the adsorption intensity. Q_{DR} (mg g^{-1}) is the saturated adsorption capacity of the D-R model, β (mol^2 J^{-2}) is the D-R constant related to the adsorption free energy and ε (J

mol^{-1}) is the Polanyi potential, T (K) and R (8.314 J mol^{-1} K^{-1}) are absolute temperature and gas constant, respectively.

Table S3 Isotherm parameters for adsorption of U(VI) of LDH FHS and C_3N_4-HCS@LDH composite.

Materials	T (K)	Langmuir			Freundlich			Dubinin-Radushkev	
		Q_m (mg g^{-1})	b (L mg^{-1})	R^2	k (L mg^{-1})	n	R^2	Q_{DR} (mg g^{-1})	R^2
LDH FHS	298	343.3	0.019	0.998	33.72	2.41	0.937	263.9	0.791
	308	504.4	0.046	0.999	75.78	2.97	0.837	396.6	0.821
	318	645.4	0.053	0.999	85.52	2.51	0.872	488.4	0.835
C_3N_4-HCS@LDH	298	618.6	0.045	0.998	77.41	2.30	0.901	394.0	0.653
	308	827.9	0.071	0.996	113.29	2.21	0.913	488.7	0.689
	318	939.2	0.250	0.999	224.88	2.46	0.821	589.9	0.780

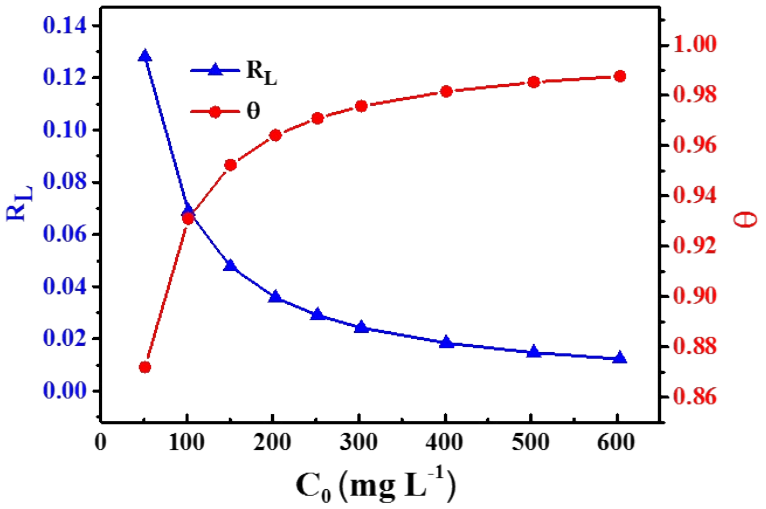

Fig. S5 Langmuir surface coverage rate (θ) and separation factor (R_L) plots of LDH FHS.

ESI.9 Effect of co-existing ions on C_3N_4-HCS@LDH

The medium for competing ions experiments was deionized water. The original concentration of Sr, Ba, Ca, Ni, Co, Na, Mg, Zn and K was listed in the **Table S4**, which was 1:1 with U (molar rate). "Volume", "temperature", "mass" and "time"

were 20 mL, 298 K, 0.01 g and 12 h, respectively.

Table S4. The original concentrations of the competing ions.

Ions	Ba	Ca	Co	K	Mg	Na	Ni	Sr	Zn
C_0 (mg L^{-1})	56.35	17.15	24.95	17.87	11.07	14.71	26.83	37.00	22.94

Table S5 The selectivity coefficients (K_d) of various ions.

Ions	Ba	Ca	Co	K	Mg	Na	Ni	Sr	Zn	U
$K_{d\text{-}C3N4\text{-}HCS@LDH}$	271	413	195	341	322	147	143	122	80	20966

ESI.10 The reusability and stability investigations

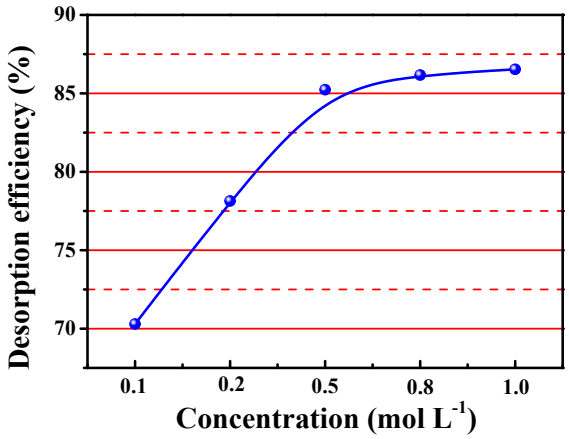

Fig. S6 The desorption efficiency for the removal of U(VI) by using different concentrations of Na_2CO_3 solution.

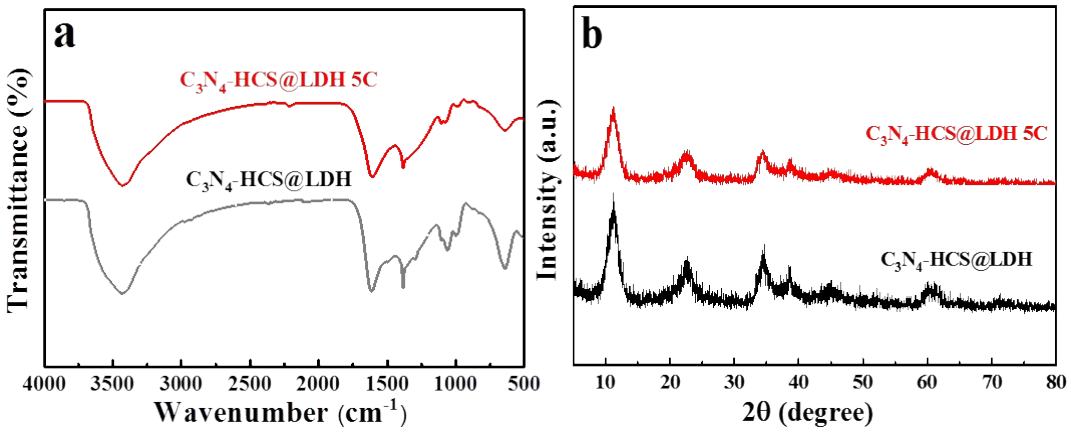

Fig. S7 The FT-IR (a) and XRD (b) patterns of C_3N_4-HCS@LDH before and after 5 adsorption-desorption cycles.

References

1. X. Zhang, L. Ji, J. Wang, R. Li, Q. Liu, M. Zhang and L. Liu, *Colloids Surf. Physicochem. Eng. Aspects*, 2012, **414**, 220-227.
2. X. Zhang, J. Wang, R. Li, Q. Dai, R. Gao, Q. Liu and M. Zhang, *Ind. Eng. Chem. Res.*, 2013, **52**, 10152-10159.
3. W. Li, R. Chen, Q. Liu, J. Liu, J. Yu, H. Zhang, R. Li, M. Zhang and J. Wang, *ACS Sustain. Chem. Eng.*, 2018, **6**, 13385-13394.
4. H. Liu, M. Li, T. Chen, C. Chen, N. S. Alharbi, T. Hayat, D. Chen, Q. Zhang and Y. Sun, *Environ. Sci. Technol.*, 2017, **51**, 9227-9234.
5. X. Wang, S. Yu, Y. Wu, H. Pang, S. Yu, Z. Chen, J. Hou, A. Alsaedi, T. Hayat and S. Wang, *Chem. Eng. J.*, 2018, **342**, 321-330.
6. C. Zhang, Y. Liu, X. Li, H. Chen, T. Wen, Z. Jiang, Y. Ai, Y. Sun, T. Hayat and X. Wang, *Chem. Eng. J.*, 2018, **346**, 406-415.

7. W. Long, H. Liu, X. Yan and L. Fu, *IOP Conf. Ser.: Mater.Sci. Eng,* 2018, **322**, 022019.